# Controlling synchrony in oscillatory networks via an act-and-wait algorithm

Irmantas Ratas[1] and Kestutis Pyragas[1,2]
[1]*Center for Physical Sciences and Technology, A. Goštauto 11, LT-01108 Vilnius, Lithuania*
[2]*Department of Theoretical Physics, Faculty of Physics, Vilnius University, LT-10222 Vilnius, Lithuania*
(Received 10 March 2014; published 15 September 2014)

The act-and-wait control algorithm is proposed to suppress synchrony in globally coupled oscillatory networks in the situation when the simultaneous registration and stimulation of the system is not possible. The algorithm involves the periodic repetition of the registration (wait) and stimulation (act) stages, such that in the first stage the mean field of the free system is recorded in a memory and in the second stage the system is stimulated with the recorded signal. A modified version of the algorithm that takes into account the charge-balanced requirement is considered as well. The efficiency of our algorithm is demonstrated analytically and numerically for globally coupled Landau-Stuart oscillators and synaptically all-to-all coupled FitzHugh-Nagumo as well as Hodgkin-Huxley neurons.

DOI: 10.1103/PhysRevE.90.032914 PACS number(s): 05.45.Xt, 02.30.Yy, 02.30.Ks

## I. INTRODUCTION

Synchronization processes in large populations of interacting oscillatory elements are the focus of intense research in physical, chemical, and biological systems [1–7]. In practical applications synchronization may play a constructive role. For example, synchronization is utilized to generate strong coherent fields in coupled arrays of lasers or Josephson junctions. However, in many situations this phenomenon is undesired and should be suppressed. An illustrative example for such a situation is the lateral swing of London's Millennium Bridge caused by coherent motion of walkers on the inauguration day in the year 2000 [8]. Another example where synchronization is harmful can be found in the Internet; the network may collapse when multiple Routers synchronize their delivering events, a dysfunction known as TCP global synchronization [9].

In the brain, oscillations are a prominent feature of neuronal activity and the synchronization of oscillations is a mechanism for neural communication, which endows individual brain areas with the ability to perform specific tasks [10]. On the other hand, it was observed that the synchronous action of the thalamus and basal ganglia neurons cause a tremor to patients with Parkinson disease [11–13], whereas in the healthy state neurons act uncorrelated [14]. Electrical deep brain stimulators (DBS) have been developed and implanted in patients to discharge an electrical signal into the brain tissue and to restore the normal activity [15–18]. However, DBS may cause side effects, and its therapeutic effect may decrease over time [19,20]. Hence, there is a need for less invasive stimulation techniques [21].

Methods for the control of synchronization in oscillatory networks developed to date can be roughly subdivided into two categories: without feedback [22–24] and with feedback [25–33]. The methods without feedback are based on phase resetting principles. For example, in coordinated reset stimulation [23,24] the population of synchronized neurons is stimulated with several electrodes placed at different sites. The stimuli at different electrodes are phase shifted with respect to each other, so they entrain different synchronous clusters of neurons. When the stimulation is switched off, the clusters desynchronize. After some time the population synchronizes to the one-cluster state again, and stimulation is switched on again, and so forth. This method is easy to implement since it does not require any online measurements. However, the method requires repetitive stimulus administration and cannot constantly maintain the desired unsynchronized state. The feedback methods are superior in this way; they can stabilize the desired unsynchronized state and maintain it constantly with minimal stimulation intensities. Different algorithms based on linear [25–27] and nonlinear [28] time-delayed feedback, linear feedback bandpass filters [29], and others [30–33] have been proposed.

In certain experimental systems, the implementation of feedback methods can meet fundamental problems. For example, in DBS the stimulation current exceeds the measured neuronal currents by several orders of magnitude, so reliable registration of neuronal activity in the presence of simultaneous stimulation can be hardly achieved [34]. To avoid this problem a feedback algorithm with a spatially separated stimulation and registration setup has been suggested in Ref. [33].

Here we propose an alternative, more efficient way to avoid the above problem by separating the stimulation and registration processes in time rather than in space. The block diagram of our algorithm is presented in Fig. 1. The control process involves the periodic repetition of two stages. In the first stage, the mean field of the free neuronal population is registered and recorded in a memory, and in the second stage, the memorized signal is processed by a controller and feeded back to the system. In fact, this algorithm utilizes a time-delayed feedback with the periodically switched-on and -off feedback gain, which in control theory is known as an act-and-wait control [35–38]. The main result of the control theory concerning this algorithm is that the time-delayed feedback with the periodically switched-on and -off control gain may be superior to the time-delayed feedback with the constant gain [35,36].

We demonstrate our algorithm for oscillatory networks in which each oscillator is coupled with other oscillators via a mean field; more complicated models that take into account the architecture of a network or delayed coupling are without the scope of this paper. The mean-field coupling models are very popular, since they admit an analytical treatment and provide a good understating of synchronization effects in real

 

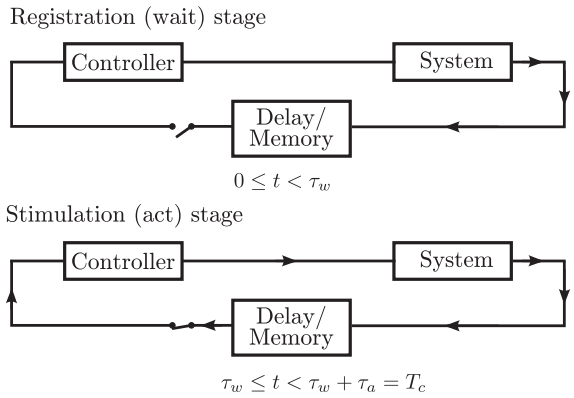


FIG. 1. Block diagram of the algorithm with the separated in time registration (wait) and stimulation (act) setup. The wait and act stages are periodically repeated with the period $T_c = \tau_w + \tau_a$, where $\tau_w$ and $\tau_a$ are the durations of the wait and act stages, respectively. In the wait stage $0 \leqslant t < \tau_w$, the mean field of the free neuronal population is recorded in a memory. In the act stage $\tau_w \leqslant t < T_c$, the system is stimulated by memorized signal, previously processed by controller.

networks (see, e.g., Refs. [8,24,25,33]). Such models enable us to investigate the performance of our algorithm by means of analytical tools.

The paper is organized as follows. In Sec. II we describe our algorithm and apply it to an ensemble of globally coupled Landau-Stuart (LS) oscillators. We present an analytical treatment of this problem in the thermodynamic limit. Section III is devoted to control of synchronization in synaptically coupled FitzHugh-Nagumo (FHN) neurons. Here we introduce a modification of our algorithm that takes into account the charge-balanced requirement. In Sec. IV we apply our algorithm to an ensemble of realistic model neurons described by Hodgkin-Huxley (HH) equations. Finally, in Sec. V we conclude this paper by discussing our results.

## II. GLOBALLY COUPLED LANDAU-STUART OSCILLATORS

To begin with, we demonstrate our algorithm for a simple model of globally coupled LS oscillators. First, we consider an analytically tractable problem when the oscillators are coupled and controlled by both dynamical variables. Then the case of coupling and control via a single variable will be considered to mimic the situation typical in neuronal systems.

### A. Coupling and control via both variables

#### 1. Model equations and control algorithm

Consider an ensemble of $N$ globally coupled and stimulated LS oscillators, representing a normal form of a supercritical Andronov-Hopf bifurcation

$$\dot{z}_j = (i\omega_j + 1 - |z_j|^2)z_j + KZ - PG(t)Z(t-\tau_a). \quad (1)$$

Here $z_j = x_j + iy_j$ is a complex-valued variable, that defines the state of the $j$-th oscillator, $j = 1,\ldots,N$. Without coupling ($K = 0$) and without stimulation ($P = 0$) each oscillator performs an uniform rotation with the natural frequency $\omega_j$ and amplitude 1. The oscillators are globally coupled via the mean field,

$$Z = \frac{1}{N}\sum_{k=1}^{N} z_k. \quad (2)$$

We suppose that both components $x$ and $y$ of the complex variable $z$ are coupled with the same coupling strength defined by the real-valued parameter $K$. The last term in Eq. (1) describes the act-and-wait control force. The delayed mean field $Z(t-\tau_a)$, which is recorded in a memory during the wait period, is multiplied by the $T_c$-periodic act-and-wait switching function

$$G(t) = \begin{cases} 0, & 0 \leqslant t < \tau_w, \\ 1, & \tau_w \leqslant t < \tau_w + \tau_a = T_c, \end{cases} \quad (3)$$

so the control force is switched off for a period of length $\tau_w$ (wait), and it is switched on for a period of length $\tau_a$ (act). The parameter $P$ defines the feedback strength, which generally can be complex valued. Here we suppose that both the real and complex parts of this parameter are available for adjustment.

In order to ensure that the stimulation is performed by a signal registered from the free (uncontrolled) system, we have to require that the act period is less or equal to the wait period $\tau_a \leqslant \tau_w$. Note that the same condition but in a different context is introduced in the theory of act-and-wait control. As pointed out in Refs. [35,36] such a condition leads to essential simplification of the time delay problem. Though the time-delayed feedback is usually associated with an infinite-dimensional phase space, the above condition allows us to treat the system as a finite-dimensional one. For $\tau_a \leqslant \tau_w$, we can reduce the problem to a finite-dimensional map that relates the state variables of the system at the beginning of the $n+1$-st control period with the state variables at the beginning of the $n$-th control period, so the stability of the controlled system is defined by eigenvalues of a finite-dimensional monodromy matrix. This differs essentially from the systems with the constant time-delayed feedback, where the analysis of the stability requires the consideration of infinite number of eigenvalues. Below we demonstrate these advantages in more detail.

In what follows we restrict ourselves to the case of equal act and wait durations $\tau_a = \tau_w \equiv \tau$. Then the period of act-and-wait switching is $T_c = 2\tau$ and the $2\tau$-periodic function $G(t)$ can be presented as

$$G(t) = H\left[-\sin(\pi t/\tau)\right], \quad (4)$$

where $H(\cdot)$ is the Heaviside step function.

#### 2. Equation for the order parameter

To explore the advantages of the act-and-wait control algorithm we investigate the phase dynamics of the system (1). Substituting $z_j = \rho_j e^{i\theta_j}$ and neglecting the dynamics of the amplitudes $\rho_j$ one can transform Eq. (1) to the following equation for the phases $\theta_j$:

$$\dot{\theta}_j = \omega_j + [Kr - PG(t)r_\tau]e^{-i\theta_j}/2i + \text{c.c.} \quad (5)$$

Here $r = r(t)$ is the complex order parameter

$$r = \frac{1}{N}\sum_{k=1}^{N} e^{i\theta_k} \quad (6)$$

and the subscript $\tau$ denotes the time-delayed value $r_\tau(t) \equiv r(t-\tau)$. The abbreviation "c.c." stands for complex conjugate. Without control ($P = 0$), Eq. (5) represents the classical Kuramoto model [1]. We assume that the frequencies $\omega_j$ are randomly distributed according to a symmetric probability density function $g(\omega)$, $g(\Omega - \omega) = g(\Omega + \omega)$, where $\Omega$ is the central frequency. Then the critical coupling for spontaneous synchronization is [1,4] $K_c = 2/\pi g(\Omega)$. For $K < K_c$ the ensemble relaxes to the state where all oscillators move incoherently, and for $K > K_c$ mutual synchronization occurs in a group of oscillators.

We now analyze the synchronization properties of the system in the presence of the act-and-wait control. We characterize the synchronization by the absolute value of the order parameter (6). The values of $|r|$ vary in the interval $[0,1]$ such that small values indicate the incoherent state while the values close to 1 represent the strong mutual synchronization. To solve the problem analytically we analyze the system (5) in the thermodynamic limit $N \to \infty$. Using the Ott-Antonsen theory [39] with the assumption that the natural frequencies $\omega_j$ satisfy the Lorentz distribution

$$g(\omega) = g_L(\omega) \equiv (\Delta/\pi)[(\omega - \Omega)^2 + \Delta^2]^{-1}, \tag{7}$$

where $\Delta$ defines the width of the distribution, the following equation for the order parameter can be derived (see Appendix A for details):

$$\dot{r} = \left[i\Omega - \Delta + \frac{K}{2}(1 - |r|^2)\right] r + \frac{G(t)}{2}(P^* r^2 r_\tau^* - P r_\tau). \tag{8}$$

This equation is considerably simpler than the original system (1) and allows for the direct analysis of the influence of the act-and-wait control on the macroscopic properties of the system. From this equation it follows that without control ($P = 0$) the order parameter $r(t)$ experiences the Andronov-Hopf bifurcation when the coupling strength $K$ is increased. For $K < K_c = 2\Delta$, the order parameter relaxes to the stable fixed point $r = 0$, which means the incoherent state of the oscillator system. When the coupling exceeds the critical value $K > K_c$, the fixed point loses the stability and $r$ approaches the stable limit cycle with the amplitude $|r| = (1 - K_c/K)^{1/2}$ and frequency $\Omega$. This corresponds to a partial synchronization, which becomes increasingly stronger when $K$ is increased. For $K \to \infty$ the systems tends to the fully synchronized state, since $|r| \to 1$. Below we analyze how this scenario changes in the presence of the act-and-wait control.

### 3. *Linear stability analysis*

We now consider an influence of the act-and-wait control on the dynamics of the order parameter defined by Eq. (8). The goal of the control is to suppress the synchronization that we assume exists in the free system due to a large global coupling, i.e., we take $K > K_c$, so the fixed point $r = 0$ of the free system is unstable. The incoherent state can be rebuilt by the control if the last term in Eq. (8) proportional to $G(t)$ stabilizes the fixed point. To analyze the stability of the fixed point we first rewrite system (8) in the rotating frame with the mean frequency $\Omega$ by changing the variable $r = e^{i\Omega t} R$. Then, linearizing the system with respect to small $R$, we obtain

$$\dot{R} = (K/2 - \Delta)\, R - G(t) P e^{-i\Omega\tau} R_\tau/2. \tag{9}$$

The change of the coordinate system does not change the absolute value of the order parameter, $|R| = |r|$. To analyze the stability of the fixed point $R = 0$ it is useful to rewrite Eq. (9) in terms of real-valued coordinates $x + iy = R$,

$$\begin{pmatrix} \dot{x} \\ \dot{y} \end{pmatrix} = \lambda \begin{pmatrix} x \\ y \end{pmatrix} - G(t) \begin{pmatrix} \bar{P}_x & -\bar{P}_y \\ \bar{P}_y & \bar{P}_x \end{pmatrix} \begin{pmatrix} x_\tau \\ y_\tau \end{pmatrix}. \tag{10}$$

Here we introduced the notations $\lambda = K/2 - \Delta > 0$, $\bar{P}_x = |P| \cos(\varphi - \Omega\tau)/2$, and $\bar{P}_y = |P| \sin(\varphi - \Omega\tau)/2$, where $\varphi$ is the argument of the complex-valued parameter $P = |P| e^{i\varphi}$.

Though the system (10) contains time delay feedback terms, which are usually associated with an infinite-dimensional phase space, it can be transformed to a finite-dimensional map (cf. Refs. [35,36]). Such a transformation is possible due to the presence of the periodic act-and-wait switching function $G(t)$. Denote the state variables of the system at the beginning of the $n$-th act-and-wait control period by $x_n = x(2\tau n)$ and $y_n = y(2\tau n)$. Then, for the wait period $2\tau n \leqslant t < 2\tau n + \tau$, the parameter $G(t) = 0$ and we obtain the solution of (10) as $x(t) = x_n e^{\lambda(t-2\tau n)}$ and $y(t) = y_n e^{\lambda(t-2\tau n)}$. In the next act period $2\tau n + \tau \leqslant t < 2\tau(n+1)$, the parameter $G(t) = 1$ so the time delay functions $x_\tau$ and $y_\tau$ come into play. These functions are exactly the above solutions obtained in the wait stage, so here Eq. (10) represents a linear nonautonomous system. Solving this system, we find the values of the state variables at the end of the act stage and finally obtain the map

$$\begin{pmatrix} x_{n+1} \\ y_{n+1} \end{pmatrix} = A \begin{pmatrix} x_n \\ y_n \end{pmatrix}, \tag{11}$$

where

$$A = e^{\lambda\tau} \begin{pmatrix} -\tau \bar{P}_x + e^{\lambda\tau} & \tau \bar{P}_y \\ -\tau \bar{P}_y & -\tau \bar{P}_x + e^{\lambda\tau} \end{pmatrix} \tag{12}$$

is the monodromy matrix. The eigenvalues $\mu_{1,2}$ of this matrix defined by the characteristic equation

$$\det(A - I\mu) = 0 \tag{13}$$

are responsible for the stability of the system (10). The origin of this system is stable if the both eigenvalues are inside the unit circle in the complex plane, $|\mu_{1,2}| < 1$. From Eqs. (12) and (13) we obtain

$$|\mu_{1,2}| = e^{\lambda\tau} \left[(\tau \bar{P}_x - e^{\lambda\tau})^2 + \tau^2 \bar{P}_y^2\right]^{1/2}. \tag{14}$$

Thus, despite the presence of time-delayed feedback, the stability of the system is defined by only two eigenvalues. By appropriate choice of the two control parameters $\bar{P}_x$ and $\bar{P}_y$ the both eigenvalues can be easily placed inside the unit circle. As is seen from Eq. (14) the parameter $\bar{P}_y$ plays a destructive role; it can only enhance the values of $|\mu_{1,2}|$. Thus the best choice is to make it zero, $\bar{P}_y = 0$. In terms of the initial complex-valued parameter $P$ this means that we fix its argument at $\varphi = \Omega\tau$, i.e., choose the feedback strength in the form $P = |P| e^{i\Omega\tau}$. Then, on substitution of $\bar{P}_x = |P|/2$ and $\bar{P}_y = 0$ into Eq. (14), the criterion of the stability simplifies to

$$|\mu_{1,2}| = |e^{\lambda\tau} - |P|\tau/2| e^{\lambda\tau} < 1.$$

From this it follows that the the act-and-wait control force can stabilize the incoherent state of strongly coupled ($K > K_c$) LS oscillators if the feedback strength satisfies the inequalities

$$P_{\rm mn} < |P| < P_{\rm mx}, \tag{15}$$

$$P_{\rm mx,mn} = 2[e^{(K/2-\Delta)\tau} \pm e^{(-K/2+\Delta)\tau}]/\tau. \tag{16}$$

The optimal value of the feedback strength is attained at $|P| = 2e^{\lambda\tau}/\tau$, when both eigenvalues vanish $|\mu_{1,2}| = 0$ and the incoherent state becomes superstable.

#### *4. Numerical simulations*

To demonstrate the efficacy of the act-and-wait control algorithm and verify the validity of the above analytical theory we have numerically simulated an ensemble of $N = 1000$ globally coupled Landau-Stuart oscillators described by Eqs. (1). The natural frequencies $\omega_j$ were randomly chosen from the Lorentzian distribution (7) with $\Omega = 0.25\pi$ and $\Delta = 0.1$. The coupling strength was taken far above the critical value of the spontaneous synchronization, $K = 0.5 > K_c = 2\Delta = 0.2$. In this case Eq. (8) predicts a rather large stationary value of the order parameter of the uncontrolled system, $|r| = (1 - K_c/K)^{1/2} \approx 0.77$. In Fig. 2(a), the dynamics of the order parameter (6) computed by direct integration of the system (1) is presented by blue (dark) curve. For $t < 100$, the control is not activated and the order parameter fluctuates with a small amplitude around the predicted value $|r| = 0.77$. When the act-and-wait control is switched on ($t \geqslant 100$) the oscillator system suddenly approaches the incoherent state and the value of the order parameter falls to zero. In the same figure, we also show [by the red (gray) curve] the dynamics of the order parameter obtained from the macroscopic Eq. (8). We see that the solution of this equation reproduces well the results obtained from the direct integration of the oscillator system (1). This confirms the validity of Ott-Antonsen ansatz (A6), which allowed us to find an analytical solution of the continuity Eq. (A2) in the presence of the act-and-wait control. In Fig. 2(b), we demonstrate how the act-and-wait control changes the dynamics of individual oscillators by taking the first three oscillators as an example.

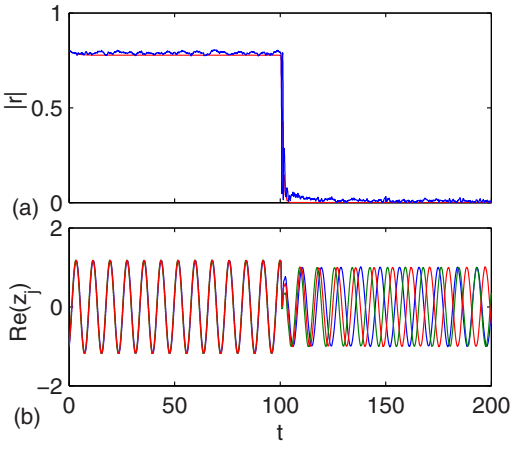


FIG. 2. (Color online) Dynamics of $N = 1000$ globally coupled Landau-Stuart oscillators (1) under act-and-wait control. For $t < 100$ the control is off ($|P|$=0), while for $t \geqslant 100$ the act-and-wait control with the feedback strength $|P| = 4$ is activated. (a) Absolute value of the order parameter estimated from direct integration of Eqs. (1) [blue (dark)] and from macroscopic Eq. (8) [red (gray)]. (b) Dynamics of the first three oscillators. The values of the parameters are as follows: $K = 0.5$, $\Omega = 0.25\pi$, $\Delta = 0.1$, and $\tau = 0.4$. The complex feedback strength is chosen in the form $P = |P|e^{i\Omega\tau}$.

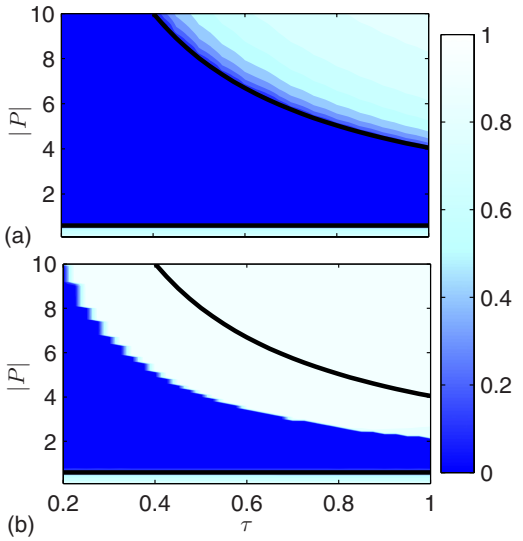


FIG. 3. (Color online) Incoherent state stability domains in the plane of parameters ($\tau$, $|P|$) for the Landau-Stuart oscillators (1) controlled by the act-and-wait algorithm. The thick black curves represent the boundaries of stability $P_{\rm mx,mn}(\tau)$ defined by Eqs. (16). The color encodes the absolute value $|r|$ of the order parameter estimated from (a) Eq. (8) and (b) Eqs. (1). The values of the parameters are as follows: $N = 1000$, $K = 0.5$, and $\Delta = 0.1$. The computations are performed in the rotating coordinate frame where $\Omega = 0$.

Incoherent state stability domains in the plane of parameters ($\tau$, $|P|$) are presented in Fig. 3. The linear theory predicts the domain of stability lying between two thick black curves $P_{\rm mx,mn}(\tau)$ defined by Eqs. (15) and (16). In Figs. 3(a) and 3(b), the values of the order parameter evaluated from the solutions of Eqs. (8) and (1), respectively, are encoded in color. We see that the linear theory predicts well the results obtained from solution of the nonlinear Eq. (8) for the order parameter. However, the prediction for the original system (1) of LS oscillators is limited. Here the linear theory predicts well only the lower boundary $|P| = P_{\rm mx}(\tau)$ of the stability domain, but with the increase of $|P|$ the oscillators start to synchronize before $|P|$ reaches the upper boundary $|P| = P_{\rm mx}(\tau)$. Such a discrepancy between the results obtained from Eqs. (1) and (8) is explained by the fact that for large $|P|$ the act-and-wait control force influences not only the phases of the individual oscillators but the amplitudes as well. Therefore, for large $|P|$ we cannot neglect the dynamics of the amplitudes and substitute the original system (1) by the Kuramoto model (5) that takes into account only the dynamics of the phases.

### B. Coupling and control via a single variable

We now consider a situation typical for neuronal systems where the interaction between neurons is provided by a

single variable, the membrane potential, while the other (gate) variables do not participate directly in the interaction. Electrical stimulation acts directly also only on the membrane potential of neurons. We can mimic this situation by modifying the system (1) as follows:

$$\dot{z}_j = (i\omega_j + 1 - |z_j|^2)z_j + K\mathrm{Re}Z - PG(t)\mathrm{Re}Z(t-\tau). \tag{17}$$

Here, unlike in Eqs. (1), the term of the global coupling and the act-and-wait control force are applied only to the real part of LS equations. We assume that both, the coupling strength $K$ and the feedback strength $P$, are real-valued parameters.

Similarly as in Sec. II A 2, we neglect the dynamics of the amplitudes and derive an equation for the phases,

$$\dot{\theta}_j = \omega_j - \sin(\theta_j)\mathrm{Re}\left[Kr - G(t)Pr_\tau\right]. \tag{18}$$

Now assuming that the natural frequencies are distributed by the Lorentzian law (7) and repeating the procedure presented in Appendix A, one can show that in the thermodynamic limit $N \to \infty$, the order parameter obeys the equation

$$\dot{r} = (i\Omega - \Delta)r + \frac{1-r^2}{2}\left[K\mathrm{Re}(r) - G(t)P\mathrm{Re}(r_\tau)\right]. \tag{19}$$

To analyze the stability of the incoherent state $r = 0$, we rewrite Eq. (19) in terms of real-valued coordinates $x + iy = r$ and, linearizing it with respect to the fixed point $(x, y) = (0, 0)$, obtain

$$\begin{pmatrix}\dot{x}\\ \dot{y}\end{pmatrix} = \begin{pmatrix}K/2-\Delta & -\Omega\\ \Omega & -\Delta\end{pmatrix}\begin{pmatrix}x\\ y\end{pmatrix} - G(t)\frac{P}{2}\begin{pmatrix}x_\tau\\ 0\end{pmatrix}. \tag{20}$$

From this it follows that the incoherent state of the control-free ($P = 0$) system is unstable for $K > K_c = 4\Delta$. We suppose that this inequality is fulfilled and look for the act-and-wait control parameters $(\tau, P)$, which lead to the stabilization of the zero fixed point of the system (20). As well as in Sec. II A 2, an analytical solution of this system can be written in the form of Eq. (11). However, an expression for the monodromy matrix is now much more complicated and we do not present it here. Generally, analytical expressions for the stability domains in the $(\tau, P)$ plane are not available, but they can be easily estimated numerically.

An exception where an analytical result can be gained is the case of small $\tau$. As is shown in Appendix B, for $\tau \to 0$, the system (17) can be treated by the method of averaging and its solution can be approximated as $z_j \approx \bar{z}_j$, where $\bar{z}_j$ satisfy the averaged equations

$$\dot{\bar{z}}_j = (i\omega_j + 1 - |\bar{z}_j|^2)\bar{z}_j + (K - P/2)\mathrm{Re}\bar{Z} \tag{21}$$

with $\bar{Z} = N^{-1}\sum_{j=1}^{N}\bar{z}_j$. By comparison of Eqs. (21) and (17) we see that for $\tau \to 0$ the act-and-wait control transforms to the proportional feedback control. On the other hand, Eq. (21) can be treated as a control-free equation but with the modified coupling strength $K \to K - P/2$. Then, from Eq. (20), we obtain a simple criterion for the stability of the incoherent state,

$$P > 2(K - 4\Delta). \tag{22}$$

The results of numerical simulations of Eqs. (17) and (19) and the linear stability analysis based on Eq. (20) are presented in Figs. 4 and 5. In Fig. 4, we choose the values of the parameters $\Delta = 0.1$ and $K = 1 > K_c = 0.4$ so the control-free system is synchronized ($|r| \approx 0.78$) and show that the switching on of the act-and-wait control leads to the desynchronization characterized by a small value of the order parameter. The dynamics of the order parameter [Fig. 4(a)] obtained from Eq. (19) agree well with the results of direct simulation of Eqs. (17). In Fig. 4(b), we show the dynamics of

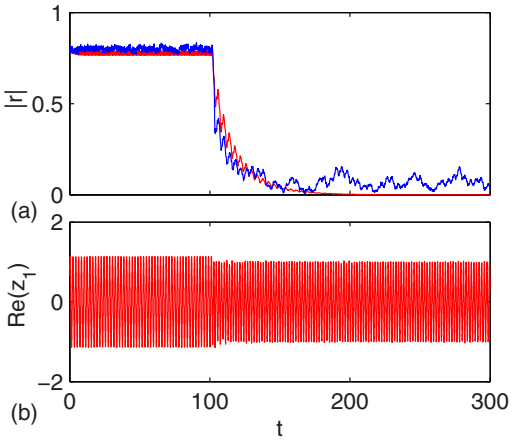


FIG. 4. (Color online) Dynamics of globally coupled $N = 1000$ Landau-Stuart oscillators (17) under act-and-wait control. For $t < 100$ the control is off ($P = 0$), while for $t \geqslant 100$ the act-and-wait control with the feedback strength $P = 1.5$ is activated. (a) Absolute value of the order parameter estimated from direct integration of Eqs. (17) [blue (dark)] and from macroscopic Eq. (19) [red (gray)]. (b) Dynamics of the first oscillator. The values of the parameters are as follows: $K = 1$, $\Omega = \pi$, $\Delta = 0.1$, and $\tau = 2$.

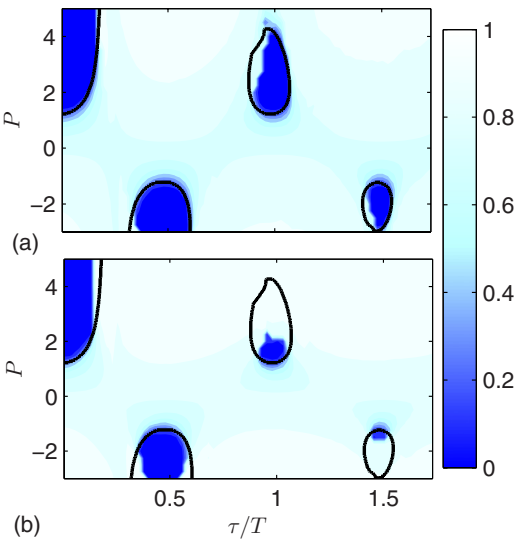


FIG. 5. (Color online) Incoherent state stability domains in the plane of parameters ($\tau$, $P$) for the Landau-Stuart oscillators (17) controlled by the act-and-wait algorithm. The thick black curves represent the boundaries of stability derived from linear Eq. (20). The color encodes the absolute value $|r|$ of the order parameter estimated from (a) Eq. (19) and (b) Eqs. (17). The values of the parameters are as follows: $N = 1000$, $K = 1$, $\Delta = 0.1$, $\Omega = \pi$, and $T = 2\pi/\Omega$.

the first oscillator. The results of the linear stability analysis are presented in Fig. 5 (thick black curves). Incoherent state stability domains in the $(\tau, P)$ plane have a resonance structure; they are located at the values of $\tau = kT/2$, where $T = 2\pi/\Omega$ is the mean natural period of the oscillators and $k = 0,1,2,\ldots$ is a non-negative integer number. The feedback strength $P$ in these domains changes the sign depending on $k$ being odd or even number. In Figs. 5(a) and 5(b) the values of the order parameter evaluated from the solutions of Eqs. (19) and (17), respectively, are encoded in color. The linear theory predicts well the results obtained from solution of the nonlinear Eq. (19); however, the prediction for the original system (17) is limited. This limitation is again due to ignoring the dynamics of oscillator amplitudes in the transition from the original system (17) to the Kuramoto model (18). Note that for the given values of the parameters, the analytical condition (22) derived for $\tau \to 0$ reads $P > 1.2$. This is in good agreement with the numerical results presented in Fig. 5.

## III. SYNAPTICALLY COUPLED FITZHUGH-NAGUMO NEURONS

### A. Model equations

We now test the efficacy of the act-and-wait control for neuronal systems. We start from a simple model of synaptically coupled FitzHugh-Nagumo [40,41] neurons

$$\dot{v}_j = f(v_j) - w_j + I_j - I_{\rm syn} - I_{\rm con}, \tag{23a}$$

$$\dot{w}_j = \varepsilon(v_j + \beta - \gamma w_j). \tag{23b}$$

Here the variable $v_j$ denotes the membrane potential and $w_j$ is the recovery variable of $j$-th neuron ($j = 1,\ldots,N$), $f(v_j) = v_j - v_j^3/3$ is the cubic source term of an ionic current, $I_j$ is a stimulus current that defines the spiking frequency of the free neuron, $I_{\rm syn}$ stands for the synaptic current of the $j$-th neuron due to connection with other neurons, and $I_{\rm con}$ is the current generated by the act-and-wait control algorithm. The constant $\varepsilon > 0$ is the ratio between the characteristic time scales of $v_j$ and $w_j$ variables. We choose the standard values of the parameters $\varepsilon = 0.2$, $\gamma = 0.8$, and $\beta = 0.7$.

In order to spread the natural spiking frequencies of neurons, the stimulus currents $I_j$ are generated by a normal distribution with the mean value $\langle I \rangle = 1$ and the standard deviation $\sigma = 0.1$. We assume that neurons are globally coupled via a synaptic current defined as

$$I_{\rm syn} = g(v_j - v_c)\frac{1}{N-1}\sum_{k\neq j}\Theta(v_k - v_0), \tag{24}$$

where $\Theta(v) = 1/[1 + \exp(-v/v_{\rm th})]$ is a sigmoid function with the characteristic threshold parameter $v_{\rm th}$ and $v_c$ is the reversal potential. We choose the parameters of synaptic current in such a way as to model an excitatory coupling; each generated spike speeds up other neurons to generate spikes, so that without control ($I_{\rm con} = 0$) the population spikes in synchrony. Then we seek to suppress the synchronization by an external current constructing in the form of the act-and-wait control,

$$I_{\rm con}(t) = G(t)PV(t-\tau), \tag{25}$$

where

$$V(t) = \frac{1}{N}\sum_{k=1}^{N} v_k(t). \tag{26}$$

is the mean field of membrane potential, which we assume is accessible for the measurement. The parameter $P$ defines the feedback strength, and the $2\tau$-periodic act-and-wait switching function $G(t)$ is defined by Eq. (4).

### B. Criteria of synchronization and numerical results

In coupled and controlled neuronal population the individual phases of neurons can be defined as follows [5]:

$$\theta_j(t) = 2\pi\frac{t - t_k^{(j)}}{t_{k+1}^{(j)} - t_k^{(j)}}, \quad t_k^{(j)} \leqslant t \leqslant t_{k+1}^{(j)}. \tag{27}$$

Here $t_k^{(j)}$ are the moments when the membrane potential of the $j$-th neuron reaches the maximum. Using this phase definition we can characterize the synchronization between neurons by the standard order parameter $r = N^{-1}\sum_{j=1}^{N} e^{i\theta_j}$. The dynamics of this characteristic for $N = 500$ synaptically coupled FHN neurons is presented in Fig. 6(a). For $t < 1500$, when the control is off ($I_{\rm con} = 0$), the value of the order parameter is close to 1. This indicates a highly synchronized state induced by synaptic interjection. Then, for $t > 1500$, the synchronization is effectively suppressed, when the control

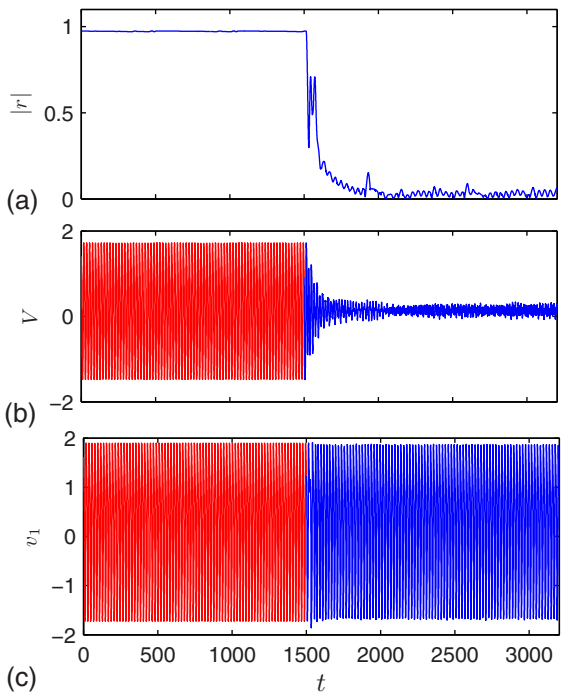


FIG. 6. (Color online) Dynamics of $N = 500$ synaptically coupled FitzHugh-Nagumo neurons (23) under act-and-wait control. For $t < 1500$ the control is off ($I_{\rm con} = 0$), while for $t \geqslant 1500$ the act-and-wait control (25) with the parameters $\tau = 18.5$ and $P = 0.2$ is activated. (a) Absolute value of the order parameter; (b) the mean field of membrane potential (26); and (c) the membrane potential of the first neuron. The values of the parameters are as follows: $\varepsilon = 0.2$, $\beta = 0.7$, $\gamma = 0.8$, $v_0 = 1$, $v_c = 2.8$, $g = 0.05$, and $v_{\rm th} = 0.1$.

current (25) with appropriate values of the parameters $\tau = 18.5$ and $P = 0.2$ is switched on. Here the order parameter falls to values close to zero. The effect of synchronization suppression is also observed in the dynamics of the mean field (2) presented in Fig. 6(b). When neurons are synchronized ($t < 1500$), the mean field oscillates with an amplitude comparable to the amplitude of individual neurons, but incoherently spiking neurons ($t > 1500$) produce mean-field oscillations with a small amplitude. In order to demonstrate that the act-and-wait control does not destroy the spiking of individual neurons, in Fig. 6(c) we show the dynamics of the first neuron, as an example.

The phase definition (27) is not universal and its use becomes problematic when the dynamics of individual neurons is complex. Such a complex dynamics appears, e.g., for the values of the act-and-wait control parameters that do not succeed in the desynchronization. Thus for more detailed analysis of outcomes of the act-and-wait control algorithm we need an alternative, more universal, criterion of synchronization. Below we use the criterion based on the comparison of mean fields of the controlled and uncontrolled systems as follows [42]:

$$S = [\mathrm{Var}(V_{\mathrm{stim}})/\mathrm{Var}(V_{\mathrm{free}})]^{1/2}. \qquad (28)$$

The parameter $S$ is defined as the square root of the ratio between the variances of the mean fields of the controlled $\mathrm{Var}(V_{\mathrm{stim}})$ and control-free $\mathrm{Var}(V_{\mathrm{free}})$ system. In the synchronized state, when all neurons spike simultaneously, the value of this parameter is close to 1, while in the incoherent state it is close to zero.

In Fig. 7(a), we present the results of numerical computation of the parameter $S$ in the dependence of the act-and-wait control parameters $\tau$ and $P$. The values of $S$ in the $(\tau, P)$ plane are depicted in color code. We see that the incoherent state domains have a resonance structure similar to that obtained for the Landau-Stuart oscillators (see Fig. 5). They are located at $\tau = kT/2$, where $T \approx 19.8$ is the period of the mean-field oscillations of the coupled control-free neurons and $k = 0,1,2,\ldots$ is a nonnegative integer number. The odd $k$ defines the domains with positive values of $P$, while the even $k$ corresponds to the negative $P$.

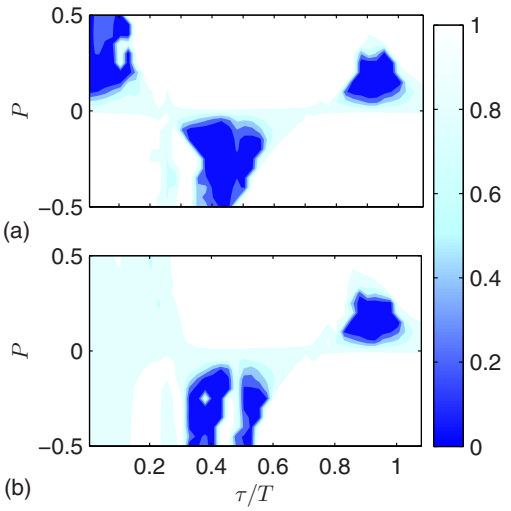


FIG. 7. (Color online) Performance of the act-and-wait control algorithm for synaptically coupled FHN neurons (23): (a) control law (25) without charge-balanced requirement and (b) control law (30) with the charge-balanced requirement. The color in the $(\tau, P)$ parameter plane encodes the value of the synchronization criterion $S$ defined by Eq. (28). Incoherent states are characterized by small values of $S$. The period of the mean-field oscillations of the coupled control-free neurons is $T \approx 19.8$ and other parameters are the same as in Fig. 6.

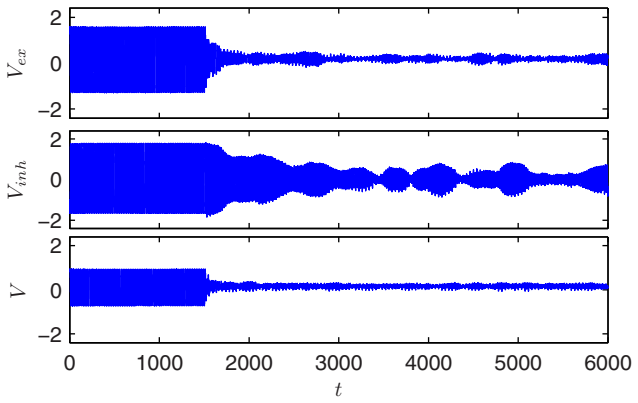


FIG. 8. (Color online) Mean fields of the membrane potential of $N_{\mathrm{ex}} = 400$ excitatory and $N_{\mathrm{inh}} = 100$ inhibitory globally coupled by synaptic links FitzHugh-Nagumo neurons (23) under act-and-wait control. The top and middle panels represent mean fields of excitatory and inhibitory neurons, respectively, while the bottom shows the total mean field. All except the coupling parameters are the same as in Fig. 6: $g = 0.1$, $v_c = 2.8$ for excitatory and $v_c = -2.8$ for inhibitory coupled neurons.

We also verified our algorithm for a network that contains both the excitatory and inhibitory coupling. The inhibitory coupling is modeled with the same expression for a synaptic current (24) as for the excitatory coupling, but the values of the parameters $v_c$ and $g$ differ. The reversal potential $v_c$ for the inhibitory coupling is chosen in such a way that the synaptic current slows down the action potential of a neuron. In Fig. 8 we present the results of simulation of a network of $N = N_{\mathrm{ex}} + N_{\mathrm{inh}} = 500$ globally coupled FHN neurons, $N_{\mathrm{ex}} = 400$ neurons of which are coupled excitatory and $N_{\mathrm{inh}} = 100$ neurons are coupled inhibitory. Without control ($t < 1500$), two synchronization clusters emerge, which contain the neurons with only excitatory and only inhibitory coupling. The mean fields of neurons with the excitatory and inhibitory couplings and the total mean field are shown in the figure from top to bottom, respectively. The decrease of all these mean fields after switching on ($t > 1500$) of the control shows that our algorithm is capable to desynchronize a network with a mixed excitatory and inhibitory coupling.

### C. Charge-balanced stimulation

In practice, electrical neuron stimulation algorithms require some additional constraints. One of them is that the control current has not to accumulate charge in the cell, i.e., the control current integrated over the period of stimulation has to vanish. This so-called charge-balanced stimulation requirement is clinically mandatory to avoid tissue damage [43,44]. Such a requirement can be easily satisfied by a simple modification

of the act-and-wait control algorithm as follows. For each $n$-th wait stage we estimate the mean value of the recorded signal,

$$\bar{V}_n = \frac{1}{\tau}\int_{2n\tau}^{(2n+1)\tau} V(t)dt, \tag{29}$$

and then in the following act stage we subtract this value from the recorded signal, i.e., instead of the control current (25) we apply the current in the following form:

$$I_{\rm con}(t) = G(t)P[V(t-\tau) - \bar{V}_n]. \tag{30}$$

As is seen from Fig. 7(b) this algorithm is successful as well as the algorithm without charge-balanced requirement, whose performance is presented in Fig. 7(a). The only qualitative effect induced by the charge-balanced requirement is that the act-and-wait control technique stops working for small values of $\tau$. Comparing Figs. 7(a) and 7(b) we see that the domain of successful desynchronization at small $\tau$ exists in Fig. 7(a) and disappears in Fig. 7(b). An explantation of this effect is given in the Appendix B.

## IV. HODGKIN-HUXLEY NEURONS UNDER CHARGE-BALANCED ACT-AND-WAIT CONTROL

As a last example demonstrating the efficacy of our algorithm we consider synchronization control in an ensemble of synaptically coupled realistic model neurons described by the Hodgkin-Huxley equations [45],

$$\begin{aligned} C\dot{v}_j &= -g_{Na}m_j^3h_j(v_j - v_{Na}) - g_Kn_j^4(v_j - v_K) \\ &\quad - g_L(v_j - v_L) + I_j + I_{\rm syn} + I_{\rm con}, && \text{(31a)}\\ \dot{m}_j &= \alpha_m(v_j)(1-m_j) - \beta_m(v_j)m_j, && \text{(31b)}\\ \dot{h}_j &= \alpha_h(v_j)(1-h_j) - \beta_h(v_j)h_j, && \text{(31c)}\\ \dot{n}_j &= \alpha_n(v_j)(1-n_j) - \beta_n(v_j)n_j. && \text{(31d)} \end{aligned}$$

Here $v_j$ is the membrane potential of the $j$-th neuron ($j = 1,\ldots,N$) measured in mV. We take the standard values of the parameters that have been obtained by fitting this model to the experimental data on the giant axon of the squid [45], $C_m = 1\ \mu\text{F/cm}^2$, $(v_L, v_K, v_{Na}) = (10.6, -12, 115)$ mV, $(g_L, g_K, g_{Na}) = (0.3, 36, 120)$ mS/cm$^2$. The rate parameters defining the dynamics of the gating variables $m_j$, $h_j$, and $n_j$ measured in ms$^{-1}$ are the following functions of the membrane potential:

$$\begin{aligned} \alpha_m(v_j) &= (2.5 - 0.1v_j)/[\exp(2.5 - 0.1v_j) - 1], && \text{(32a)}\\ \beta_m(v_j) &= 4\exp(-v_j/18), && \text{(32b)}\\ \alpha_h(v_j) &= 0.07\exp(-v_j/20), && \text{(32c)}\\ \beta_h(v_j) &= 1/[\exp(3 - 0.1v_j) + 1], && \text{(32d)}\\ \alpha_n(v_j) &= (0.1 - 0.01v_j)/[\exp(1 - 0.1v_j) - 1], && \text{(32e)}\\ \beta_n(v_j) &= 0.125\exp(-v_j/80). && \text{(32f)} \end{aligned}$$

The voltage scale in this model is shifted in such a way that the membrane resting potential (i.e., the steady state value of the membrane potential without external currents, $I_j = I_{\rm syn} = I_{\rm con} = 0$) is zero.

The spiking regimes of individual neurons are induced by direct stimulation currents $I_j$. In order to spread the natural spiking frequencies of neurons we choose these values randomly from a normal distribution with the mean $\langle I\rangle = 25\ \mu\text{A/cm}^2$ and standard deviation $\sigma = 0.5\,\mu\text{A/cm}^2$. The neurons are globally coupled via synaptic current $I_{\rm syn}$ defined by Eq. (24) with the parameters $(v_c, v_0, v_{\rm th}) = (120, 50, 10)$ mV/cm$^2$. The charge-balanced act-and-wait control is performed via the current $I_{\rm con}$ determined by Eq. (30).

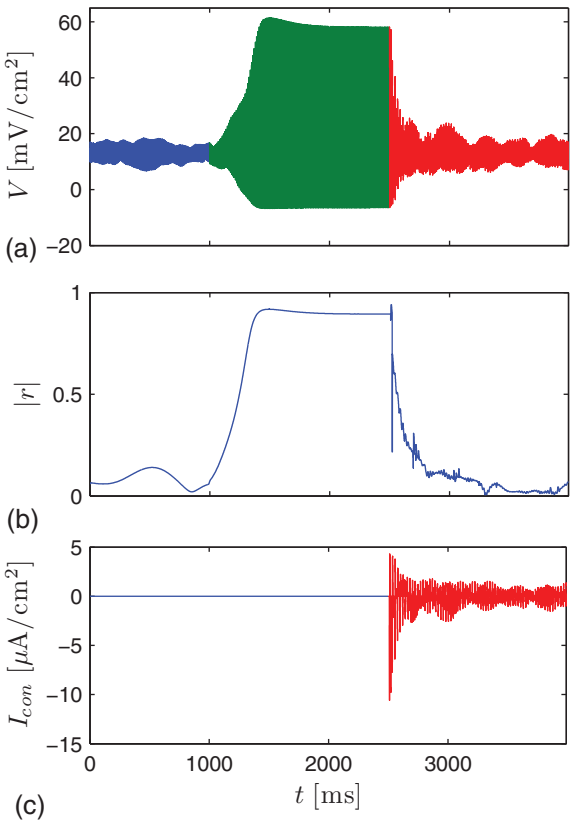


FIG. 9. (Color online) Dynamics of an ensemble of $N = 100$ Hodgkin-Huxley neurons (31). In the time interval $t \in [0,1000]$ ms the control and coupling are off ($g = 0$, $P = 0$). In the interval $t \in [1000,2500]$ ms the synaptic coupling (24) with the strength $g = 0.05$ mS/cm$^2$ is activated but the control is off. For $t \geqslant 2500$ ms the charge-balanced act-and-wait control (30) with the strength $P = 0.23$ mS/cm$^2$ and delay time $\tau = 10.5$ ms is activated. (a) The mean field of membrane potential, (b) absolute value of the order parameter, and (c) the control current.

In Fig. 9 we show the results of numerical simulation of system (31) for $N = 100$ neurons. In the time interval $t \in [0,1000]$ ms the dynamics of uncoupled ($g = 0$) and uncontrolled ($P = 0$) neurons is presented. Then in the interval $t \in [1000,2500]$ ms the synaptic coupling (24) with the strength $g = 0.05$ mS/cm$^2$ is activated but the control is off. Finally, for $t \geqslant 2500$ ms we activate the charge-balanced act-and-wait control (30) with the strength $P = 0.23$ mS/cm$^2$ and delay time $\tau = 10.5$ ms. We see that the mean field $V$ of uncoupled and uncontrolled neurons fluctuates with a small amplitude about some mean value [Fig. 9(a)] and the order parameter $|r|$ is small [Fig. 9(b)]. When the synaptic coupling is switched on, the neurons synchronize and the amplitude of the mean field as well as the order parameter increase. This synchronization is effectively suppressed when the control

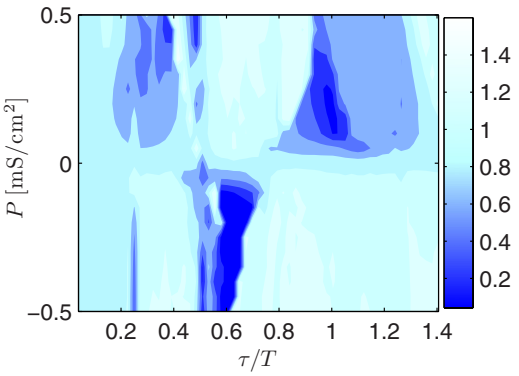


FIG. 10. (Color online) Performance of the charge-balanced act-and-wait control algorithm for synaptically coupled Hodgkin-Huxley neurons (31). The color in the $(\tau, P)$ parameter plane encodes the value of the synchronization criterion $S$ defined by Eq. (28). Incoherent states are characterized by small values of $S$. The period of the mean-field oscillations of the coupled control-free neurons is $T \approx 10.5$ ms. The values of the parameters are the same as in Fig. 9.

is switched on. The amplitude of the mean field suddenly decreases and we observe the fluctuations of the mean field similar to those observed without coupling and control. The order parameter also falls suddenly to small values. In Fig. 9(c), we show the dynamics of the control current. When the system is desynchronized, the control current does not vanish. This is conditioned by the mean-field fluctuations that remain in the desynchronized state due to the finite number of neurons. Here we do not show the dynamics of individual neurons, because it is analogous to that observed in the FHN model; the control does not destroy the spiking of individual neurons.

In Fig. 10, we present the results of numerical computation of the synchronization criterion (28) in the dependence of the act-and-wait control parameters $\tau$ and $P$. The values of the parameter $S$ in the ($\tau$, $P$) plane are depicted in color code. The incoherent state domains have again the resonance structure similar to that obtained for the FHN neurons [see Fig. 7(b)]. Note that here as well as for the FHN neurons the charge-balanced act-and-wait control fails for $\tau \to 0$ (see the Appendix B for details).

## V. DISCUSSION

We have proposed an algorithm for synchrony suppression in ensembles of globally coupled oscillators for a complicated control situation, when an output signal is small in comparison to a stimulated signal so reliable simultaneous registration and stimulation of the system is not possible and the standard feedback control algorithms cannot be applied. Such a situation is typical, e.g., for neuronal systems. Our algorithm is based on the act-and-wait control, which assumes a separation in time the registration and stimulation stages. In the registration (wait) stage, the mean field of the free oscillatory system is recorded in a memory and in the stimulation (act) stage it is feeded back to the system. We assume that the duration of the act stage is less or equal to the duration of the wait stage. The periodic repetition of these two stages can effectively destroy the mutual synchronization in ensembles of globally coupled oscillators. Mathematically, this algorithm is described by delay differential equations with the periodically switched-on and -off time-delay feedback term. Although systems with time delay are usually associated with an infinite-dimensional phase space, here the problem of stability of the incoherent state is definite by the eigenvalues of a finite-dimensional monodromy matrix. This fact facilitates considerably the search for appropriate control parameters that guarantee the stability of the incoherent state.

The efficacy of our algorithm is demonstrated analytically and numerically with several examples. As the first example we consider an ensemble of globally coupled Landau-Stuart oscillators. We reduce this system to a Kuramoto model, and in the thermodynamic limit, derive a macroscopic equation for the order parameter. In the case when coupling and control is performed through both variables, we obtain a simple analytical criterion for the stability of the incoherent state. Then the case of coupling and control through a single variable is considered in order to mimic a situation typical for neuronal systems. We show that the incoherent state stability domains in the $(\tau, P)$ parameter plane (where $\tau$ is the duration of act and wait periods, and $P$ is the feedback strength) have a resonance structure; they are located at the values of $\tau = kT/2$, where $T$ is the characteristic period of oscillations of the mean field of synchronized oscillators in the absence of control and $k$ is a non-negative integer number.

The analysis of more complicated systems such as ensembles of synaptically coupled FitzHugh-Nagumo or Hodgkin-Huxley neurons shows that the above resonance structure is universal. For these systems we consider a modification of the act-and-wait control algorithm that takes into account the charge-balanced requirement. This requirement is clinically mandatory to avoid tissue damage. We show that the charge-balanced requirement does not destroy the resonance structure of the incoherent state stability domains in the $(\tau, P)$ plane, but the algorithm stops to work for small values of $\tau$.

Our algorithm, which separates the registration and stimulation processes in time, is superior to the algorithm proposed in Ref. [33], where these processes are separated in space. This is because the spatial separation does not guarantee the total exclusion of the influence of the stimulation signal on the measurements of neuronal activity. Moreover, our algorithm admits a handy experimental implementation, since both the stimulation and registration processes can be served with a single electrode.

In this paper, we tested our algorithm for neural networks whose local connectivity admits the description via the mean-field approximation. In such an approximation, our algorithm is robust, since it works for networks constructed from different oscillator models, including simple Landau-Stuart oscillators, FitzHugh-Nagumo neurons as well as realistic Hodgkin-Huxley neuron models. An extension of our algorithm for more complicated networks that take into account the specific architecture or delayed coupling is the subject of our future research.

## ACKNOWLEDGMENTS

This research was funded by the European Social Fund under the Global Grant measure (Grant No. VP1-3.1-ŠMM-07-K-01-025).

## APPENDIX A: DERIVATION OF THE ORDER PARAMETER EQUATION

In this Appendix, we analyze an ensemble (5) of $N$ globally coupled LS oscillators under act-and-wait control in the thermodynamic limit $N \to \infty$. Assuming the Lorenz distribution (7) for the natural frequencies we show that the dynamics of the complex order parameter (6) satisfy a simple first-order ordinary differential equation.

In the limit $N \to \infty$, the ensemble (5) at time $t$ can be described by a continuous distribution function, $f(\omega,\theta,t)$, in frequency $\omega$ and phase $\theta$ that satisfies the normalization

$$\int_0^{2\pi} f(\omega,\theta,t)d\theta = g(\omega) \tag{A1}$$

for all $t$. Since oscillators are conserved $f$ must satisfy the continuity equation

$$\frac{\partial}{\partial t} f(\omega,\theta,t) = -\frac{\partial}{\partial \theta}[f(\omega,\theta,t)v(\omega,\theta,t)], \tag{A2}$$

where the velocity $v(\omega,\theta,t)$ is defined by the right-hand side of Eq. (5),

$$v(\omega,\theta,t) = \omega + [Kr - PG(t)r_\tau]e^{-i\theta}/2i + \text{c.c.} \tag{A3}$$

In the continuum limit, Eq. (6) can be written as

$$r = \int_0^{2\pi}\int_{-\infty}^{\infty} e^{i\theta} f(\omega,\theta,t)d\omega d\theta. \tag{A4}$$

Expanding $f(\omega,\theta,t)$ in Fourier series in $\theta$ we have

$$f = \frac{g(\omega)}{2\pi}\left(1 + \left[\sum_{n=1}^{\infty} f_n(\omega,t)e^{in\theta} + \text{c.c.}\right]\right). \tag{A5}$$

Following Ott and Antonsen [39], we restrict our analysis to a special class of distribution functions defined by the ansatz,

$$f_n(\omega,t) = [\alpha(\omega,t)]^n, \tag{A6}$$

where $|\alpha(\omega,t)| \leqslant 1$ to avoid divergence of the series. Substituting this series expansion into Eqs. (A2) and (A4) we find that this special form of $f$ satisfies Eqs. (A2) and (A4) if

$$\dot\alpha = \frac{K}{2}(r^* - r\alpha^2) - i\omega\alpha + \frac{G(t)}{2}(P\alpha^2 r_\tau - P^* r_\tau^*) \tag{A7}$$

and

$$r = \int_{-\infty}^{+\infty} \alpha^*(\omega,t)g(\omega)d\omega. \tag{A8}$$

Further simplification can be gained by choosing the density distribution of the natural frequencies in the Lorentzian function form (7). This form allows us to solve the $\omega$ integral in Eq. (A8) and obtain an explicit relation $r^*(t) = \alpha(\Omega - i\Delta,t)$. Putting this result into Eq. (A7) and setting $\omega = \Omega - i\Delta$, we finally get a closed equation for the complex order parameter

$$\dot r = \left[i\Omega - \Delta + \frac{K}{2}(1 - |r|^2)\right]r + \frac{G(t)}{2}(P^* r^2 r_\tau^* - P r_\tau). \tag{A9}$$

## APPENDIX B: THE LIMIT OF SMALL $\tau$

In this Appendix, we consider the effect of the act-and-wait control algorithm in the limit $\tau \to 0$. We show that with the charge-balanced requirement the effect of the algorithm vanishes, while without charge-balanced requirement the algorithm transforms to the proportional feedback control algorithm. We demonstrate these statements for an ensemble of interacting neurons that are described by a general Hodgkin-Huxley type model,

$$\dot v_j = F_j(v_1,\ldots,v_N,\mathbf{w}_j) - I_{\text{con}}, \tag{B1a}$$

$$\dot{\mathbf{w}}_j = \mathbf{Q}_j(v_j,\mathbf{w}_j). \tag{B1b}$$

Here $v_j$ is the membrane potential of the $j$-th neuron ($j = 1,\ldots,N$). Without loss of generality we assume that the membrane capacitance is equal to 1. The function $F_j$ describes the sum of currents flowing through ion channels of the $j$-th neuron. This function includes the currents induced by interaction with other neurons, therefore it depends generally on the membrane potentials of all neurons. The last term in Eq. (B1a) is the control current defined either by Eq. (30) or Eq. (25) depending on the case of control with or without charge-balanced requirement, respectively. Equation (B1b) describes the dynamics of a recovery variable $\mathbf{w}_j$ of the $j$-th neuron. Generally, this is a vector variable. The function $\mathbf{Q}_j$ represents the ionic channel dynamics. The functions $F_j$ and $\mathbf{Q}_j$ are defined by the specific neuron model.

We start from the case of control without charge-balanced requirement. Then for $\tau \to 0$ the control current (25) up to the first order in $\tau$ can be approximated as

$$I_{\text{con}}(t) = G(t)P[V(t) + O(\tau)]. \tag{B2}$$

Substituting Eq. (B2) into Eq. (B1a) we get a nonautonomous system of ordinary differential equations with the high-frequency periodic function $G(t)$. Such a system can be treated by the method of averaging [46]. To transform our system to the standard form of equations as typically used by this method we rescale the time variable $\bar t = t/\tau$ (here $\bar t$ is the "fast" time) and obtain

$$\frac{dv_j}{d\bar t} = \tau\{F_j(v_1,\ldots,v_N,\mathbf{w}_j) - \tilde G(\bar t)P[V + O(\tau)]\}, \tag{B3a}$$

$$\frac{d\mathbf{w}_j}{d\bar t} = \tau\mathbf{Q}_j(v_j,\mathbf{w}_j). \tag{B3b}$$

Due to the small factor $\tau$, the variables $v_j$ and $\mathbf{w}_j$ vary slowly while the periodic function $\tilde G(\bar t) \equiv G(\tau\bar t) = H[-\sin(\pi\bar t)]$ oscillates fast. According to the method of averaging [46], an approximate solution of system (B3) can be obtained by averaging the right-hand side of the system over fast oscillations. Specifically, let us denote the variables of the averaged system as $(\bar v_j,\bar{\mathbf{w}}_j)$. They satisfy the following equations:

$$\frac{d\bar v_j}{d\bar t} = \frac{\tau}{2}\int_0^2 \{F_j(\bar v_1,\ldots,\bar v_N,\bar{\mathbf{w}}_j) - \tilde G(s)P\bar V\}ds, \tag{B4a}$$

$$\frac{d\bar{\mathbf{w}}_j}{d\bar t} = \frac{\tau}{2}\int_0^2 \mathbf{Q}_j(v_j,\bar{\mathbf{w}}_j)ds, \tag{B4b}$$

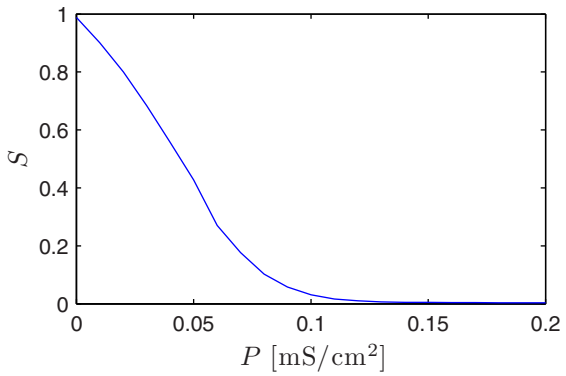


FIG. 11. (Color online) The synchronization criterion $S$ as function of the control gain $P$ for the HH model under act-and-wait control without charge-balanced requirement in the limit $\tau \to 0$. The analysis is performed by using averaged Eqs. (B5). The values of the parameters are the same as in Sec. IV.

where $\bar{V} = N^{-1}\sum_{j=1}^{N} \bar{v}_j$. The method of averaging states that the averaged system (B4) approximates the solutions of the system (B3) with the accuracy of $O(\tau)$, i.e., $v_j = \bar{v}_j + O(\tau)$ and $\mathbf{w}_j = \bar{\mathbf{w}}_j + O(\tau)$. After performing the integration [note that $\int_0^2 \tilde{G}(s)ds = 1$] and coming back to the original time scale, the averaged system (B4) takes the following form:

$$\dot{\bar{v}}_j = F_j(\bar{v}_1, \ldots, \bar{v}_N, \bar{\mathbf{w}}_j) - P\bar{V}/2, \tag{B5a}$$

$$\dot{\bar{\mathbf{w}}}_j = \mathbf{Q}_j(\bar{v}_j, \bar{\mathbf{w}}_j). \tag{B5b}$$

Here the dot denotes differentiation with respect to the original time $t$. Thus the nonautonomous system (B1) with the accuracy $O(\tau)$ can be transformed to the autonomous averaged system (B5). The last term in Eq. (B5a) describes the standard proportional feedback control with the strength $P/2$. Therefore, the act-and-wait control algorithm without charge-balanced requirement for $\tau \to 0$ transforms to the proportional feedback control algorithm.

As an example of the application of the above general results we performed the analysis of the HH model based on the averaged Eqs. (B5). The dependence of the synchronization criterion $S$ on the coupling strength $P$ presented in Fig. 11 shows that for $\tau \to 0$ the act-and-wait control algorithm without charge-balanced requirement successfully desynchronizes an ensemble of synaptically coupled HH neurons.

The consideration of the limit $\tau \to 0$ in the case of a charge-balanced requirement is much simpler. As seen from Eqs. (29) and (30), the control current in this case vanishes, $I_{\text{con}} \to 0$ as $\tau \to 0$. This explains why for $\tau \to 0$ the act-and-wait control with the charge-balanced requirement fails for both the FHN neurons [Fig. 7(b)] and the HH neurons (Fig. 10).


[1] Y. Kuramoto, *Chemical Oscillations, Waves and Turbulence* (Springer, New York, 1984).
[2] R. E. Mirollo and S. H. Strogatz, SIAM J. Appl. Math. **50**, 1645 (1990).
[3] P. Backwell, M. Jennions, and N. Passmore, Nature **391**, 31 (1998).
[4] S. H. Strogatz, Physica D **143**, 1 (2000).
[5] A. Pikovsky, M. Rosenblum, and J. Kurths, *Synchronization: A Universal Concept in Nonlinear Sciences* (Cambridge University Press, Cambridge, 2001).
[6] E. Mosekilde, Y. Maistrenko, and D. Postnov, in *Chaotic Synchronization Applications to Living Systems*, edited by L. Chua (World Scientific, Singapore, 2002).
[7] A. Arenas, A. Díaz-Guilera, J. Kurths, Y. Moreno, and C. Zhou, Phys. Rep. **469**, 93 (2008).
[8] S. H. Strogatz, D. M. Abrams, A. McRobie, B. Eckhardt, and E. Ott, Nature **438**, 43 (2005).
[9] S. R. Vegesna, *IP Quality of Service* (Cisco Press, Indianapolis, 2001).
[10] A. Schnitzler and J. Gross, Nat. Rev. Neurosci. **6**, 285 (2005).
[11] W. W. Alberts, E. W. Wright, and B. Feinstein, Nature **221**, 670 (1969).
[12] F. A. Lenz, H. C. Kwan, R. L. Martin, R. R. Tasker, J. O. Dostrovsky, and Y. E. Lenz, Brain **117**, 531 (1994).
[13] J. A. Goldberg, U. Rokni, T. Boraud, E. Vaadia, and H. Bergman, J. Neurosci. **24**, 6003 (2004).
[14] A. Nini, A. Feingold, H. Slovin, and H. Bergman, J. Neurophysiol. **74**, 1800 (1995).
[15] M. L. Kringelbach, N. Jenkinson, S. L. Owen, and T. Z. Aziz, Nat. Rev. Neurosci. **8**, 623 (2007).
[16] J. Volkmann, J. Herzog, F. Kopper, and G. Deuschl, Mov Disord. **17**, S181 (2002).
[17] C. C. McIntyre, M. Savasta, L. K.-L. Goff, and J. L. Vitek, Clin Neurophysiol. **115**, 1239 (2004).
[18] K. Pyragas, V. Novičenko, and P. A. Tass, Biol. Cybern. **107**, 669 (2013).
[19] R. Kumar, A. M. Lozano, E. Sime, and A. E. Lang, Neurology **61**, 1601 (2003).
[20] M. C. Rodriguez-Oroz, J. A. Obeso, A. E. Lang, J. L. Houeto, P. Pollak, S. Rehncrona, J. Kulisevsky, A. Albanese, J. Volkmann, M. I. Hariz, N. P. Quinn, J. D. Speelman, J. Guridi, I. Zamarbide, A. Gironell, J. Molet, B. Pascual-Sedano, B. Pidoux, A. M. Bonnet, Y. Agid, J. Xie, A.-L. Benabid, A. M. Lozano, J. Saint-Cyr, L. Romito, M. F. Contarino, M. Scerrati, V. Fraix, and N. V. Blercom, Brain **128**, 2240 (2005).
[21] P. A. Tass, *Phase Resetting in Medicine and Biology: Stochastic Modeling and Data Analysis* (Springer, Berlin, 1999).
[22] P. A. Tass, Europhys. Lett. **55**, 171 (2001).
[23] P. A. Tass, Biol. Cybern. **89**, 81 (2003).
[24] B. Lysyansky, V. O. Popovych, and P. A. Tass, J. Neural Eng. **8**, 036019 (2011).
[25] M. G. Rosenblum and A. S. Pikovsky, Phys. Rev. Lett. **92**, 114102 (2004); Phys. Rev. E **70**, 041904 (2004).
[26] C. Hauptmann, O. Popovych, and P. A. Tass, Neurocomputing **65-66**, 759 (2005); Biol. Cybern. **93**, 463 (2005).
[27] C. A. S. Batista, S. R. Lopes, R. L. Viana, and A. M. Batista, Neural Networks **23**, 114 (2010).

[28] O. V. Popovych, C. Hauptmann, and P. A. Tass, Phys. Rev. Lett. **94**, 164102 (2005); Biol. Cybern. **95**, 69 (2006); O. V. Popovych and P. A. Tass, Phys. Rev. E **82**, 026204 (2010).
[29] N. Tukhlina, M. Rosenblum, A. Pikovsky, and J. Kurths, Phys. Rev. E **75**, 011918 (2007); L. Ming, W. Yongjun, and J. Peng, Biol. Cybern. **101**, 241 (2009); G. Montaseri, M. J. Yazdanpanah, A. Pikovsky, and M. Rosenblum, Chaos **23**, 033122 (2013).
[30] B. Rosin, M. Slovik, R. Mitelman, M. Rivlin-Etzion, S. N. Haber, Z. Israe, E. Vaadia, and H. Bergman, Neuron **72**, 370 (2011).
[31] A. Berényi, M. Belluscio, D. Mao, and G. Buzsáki, Science **337**, 735 (2012).
[32] V. H. P. Louzada, N. A. M. Arajo, J. S. Andrade, Jr., and H. J. Herrmann, Sci. Rep. **2**, 658 (2012).
[33] K. Pyragas, O. Popovich, and P. Tass, Europhys. Lett. **80**, 40002 (2007).
[34] C. Beurrier, L. Garcia, B. Bioulac, and C. Hammond, Thalamus Relat. Syst. **2**, 1 (2002).
[35] T. Insperger, IEEE Transact. Control Syst. Technol. **14**, 974 (2006).
[36] G. Stépán and T. Insperger, Ann. Rev. Control **30**, 159 (2006).
[37] P. Gawthrop, IEEE Transact. Control Syst. Technol. **18**, 1195 (2010).
[38] B. Li, X. Song, and J. Zhao, Nonlinear Dynam. Syst. Theor. **13**, 171 (2013).
[39] E. Ott and T. M. Antonsen, Chaos **18**, 037113 (2008).
[40] R. A. FitzHugh, Biophys. J. **1**, 445 (1961).
[41] J. Nagumo, S. Arimoto, and S. Yoshizawa, Proc. IRE **50**, 2061 (1962).
[42] M. Rosenblum, N. Tukhlina, A. Pikovsky, and L. Cimponeriu, Int. J. Bifurcat. Chaos **7**, 1989 (2006).
[43] D. Harnack, C. Winter, W. Meissner, T. Reum, A. Kupsch, and R. Morgenstern, J. Neurosci. Methods **138**, 207 (2004).
[44] B. Piallat, S. Chabardès, A. Devergnas, N. Torres, M. Allain, E. Barrat, and A. L. Benabid, Neurosurgery **64**, 156 (2009).
[45] A. L. Hodgkin and A. F. Huxley, J. Physiol. **117**, 500 (1952).
[46] J. Sanders, F. Verhulst, and J. Murdock, *Averaging Methods in Nonlinear Dynamical Systems* (Springer, Berlin, 2007).